

# Gold Nanostructures as Photothermal Therapy Agent for Cancer

Jihye Choi<sup>1</sup>, Jaemoon Yang<sup>2</sup>, Eunji Jang<sup>1</sup>, Jin-Suck Suh<sup>2,4</sup>, Yong-Min Huh<sup>2,4</sup>, Kwangyeol Lee<sup>3,\*</sup> and Seungjoo Haam<sup>1,4,\*</sup>

<sup>1</sup>Department of Chemical and Biomolecular Engineering, Yonsei University Seoul 120-749, Republic of Korea; <sup>2</sup>Department of Radiology, Yonsei University Seoul 120-752, Republic of Korea; <sup>3</sup>Department of chemistry, Korea University Seoul 136-701, Republic of Korea; <sup>4</sup>YUHS-KRIBB Medical Convergence Research Institute, Seoul 120-752, Republic of Korea

**Abstract:** Well-designed photothermal nanostructures have attracted many scientists pursuing a better means to accurately diagnose cancer and assess the efficacy of treatment. Recently, gold-based nanostructures (nanoshells, nanorods and nanocages) have enabled photothermal ablation of cancer cells with near-infrared (NIR) light without damaging normal human tissues and in particular, animal studies and early clinical testing showed the great promise for these materials. In this review article, we first discuss the mechanism of the cellular death signaling by thermal stress and introduce the intrinsic properties of gold nanostructures as photothermal agent for cancer treatment. Then the overview follows for evolving researches for the synthesis of various types of gold nanostructures and for their biomedical applications. Finally we introduce the optimized therapeutic strategies involving nanoparticle surface modification and laser operation method for an enhanced accumulation of gold nanostructures to the target cancer as well as for an effective cancer cell ablation.

**Keywords:** Gold nanostructures, photothermal therapy, Near-IR, cancer.

## INTRODUCTION

To date, surgical resection has been employed as the widespread therapeutic method for the most cancers. There are, however, several drawbacks such as a required large incision accompanied by pains and a second operation for bilateral diseases [1]. Therefore, alternative cancer therapies (chemotherapy [2] and radiation therapy [3] either alone or in combinations [4]) have been developed for reduced pain, speedy recovery, and reduced post-surgical complications. However, these methods are not completely free of side effects [5, 6] such as hair loss, mouth sores, nausea or vomiting, skin redness and cosmetic defects because high doses of anticancer drugs and high energy X-ray can destroy or slow down the growth of normal cells. Thus, noninvasive photothermal ablation of tumor using the near-infrared (NIR) light has recently attracted attentions to selectively kill cancer cells and to prevent undesirable damages for healthy tissues [7]. On the other hand, photothermal therapy meets the requirements such as low energy at the long wavelength that allows a deep tissue penetration and accurate targeting of cancerous cells without abnormal effect to the surrounding tissue. To satisfy therapeutic needs, gold nanostructures as photothermal agents have recently emerged for promising applications [8-10]. When a NIR light is illuminated at the resonance wavelength of gold nanostructures, the absorbed energy is converted into heat, which raises the hyperthermic stress to the target cells and subsequently kills the cancer cells by the death signaling [11]. In particular, gold nanostructures have been noticed as photothermal agent in early clinical trials because the absorption band of gold nanostructures can be tuned from visible to NIR region by the controlling of size and shape. Furthermore, surface functional groups of gold nanostructures can be further modified to enhance the efficiency of a photothermal therapy.

In this review, we will cover overall strategies for photothermal cancer therapy using gold nanostructures. The mechanism for the cellular death signaling induced by a thermal stress will be

described first. Subsequently, the overview will be depicted about intrinsic properties of gold nanostructures for the photothermal ablation and imaging of cancer cells. In particular, the heat generation mechanism of gold nanostructures by the irradiated light and various gold nanostructures as effective photothermal agents will be described. Finally, methods to induce and provide photothermal energy to the cancer cells will be presented.

## 1. Hyperthermic Stress for Cancer Cell Death

In recent years, photothermal cancer therapy based on gold nanostructures has received a great attention because of a much mitigated invasiveness of the treatment in comparison with other typical therapeutic methods such as a surgical resection. To accomplish highly effective photothermal ablation of cancer cells, the understanding of the mechanism for the cellular death induced by hyperthermic stress from gold nanostructures is very important; cellular life has been derived from regulated processes which are controlled by various signal transduction pathways. For the cells under various stress conditions such as high temperature, oxidative environments and chemical compounds (i.e. heavy metals and anti-cancer drugs), the death signals were turned on and transmitted to cause cell death in most cases [12-14]. In particular, the intracellular protein-damages induced by a hyperthermic stress can inhibit the entire cellular metabolism related to the cellular survival and proliferation [15].

Signaling pathways for the cellular death are closely linked with various heat shock proteins (Hsp) as chaperones because Hsp groups (such as Hsp70 family, Hsp90 family and Hsp27) play crucial roles for the protection of a severe hyperthermic stress-induced apoptosis induced by the intracellular protein misfolding [16]. In Table 1, the detailed functions of Hsp groups are grouped into sub-families with molecular weights of approximately 10~30, 40, 60, 70, 90 and 100 kDa. Some of these such as Hsp70 and Hsp90 families regulate the productive folding of proteins and help to protect against protein misfolding and undesirable aggregations under a hyperthermic stress condition [17]. Moreover, Hsp90 family can capture and hold client proteins in intermediate conformations with refolding of denatured substrates and transfer to the Hsp70/Hsp40 chaperone machine [18]. Hsp27 inhibits protein aggregation and stabilizes denatured protein [19]. From a signaling pathway viewpoint in Fig. (1), when Hsp70 family is impaired by a hyperthermic stress, heat shock causes Bax translocation from the cytosol to mi-

\*Address correspondence to these authors at the Department of chemistry, Korea University Seoul 136-701, Republic of Korea; Tel: 82-2-3290-3139; Fax: 82-2-3290-3121; E-mail: kyleel@korea.ac.kr and Department of Chemical and Biomolecular Engineering, Yonsei University Seoul 120-749, Republic of Korea; Tel: 82-2-2123-2751; Fax: 82-2-312-6401; E-mail: haam@yonsei.ac.kr

Table 1. Major Hsp Families Related with Cellular Survival [22, 23]

| Hsp Family | Approximate Molecular Weight (kDa) | Members   | Function   | Intracellular Location                           |
|------------|------------------------------------|---|--|--|
| Small Hsps | 10 ~ 30                            | Hsp10,GroES,Hsp16, α-crystalin, Hsp20, Hsp25, Hsp27   | Prevent the aggregation of other proteins, by collecting protein“garbage”, act as “dustmen” of cells   | Cytosol  |
| Hsp40      | 40                                 | Hsp40, DnaJ, SIS1   | Co-factor of Hsp70   | Cytosol  |
| Hsp60      | 60                                 | Hsp60, Hsp65, GroEL   | Assistance in protein folding and re-folding   | Cytosol and mitochondria                         |
| Hsp70      | 70                                 | The HspA group of Hsp including Hsp71, Hsp70, Hsp72, Grp78 (BiP), Hsx70 found only in primates and DnaK | Assistance in protein folding and re-folding   | Cytosol , mitochondria and endoplasmic reticulum |
| Hsp90      | 90                                 | The HspC group of Hsp including Hsp90, Grp94, HtpG, C62.5   | Stabilize substrate proteins and maintain their active, or inactive state, prevent the aggregation of other proteins, by collecting protein “garbage”, act as “dustmen” of cells | Cytosol and endoplasmic reticulum                |
| Hsp100     | 100                                | Hsp104, Hsp110, ClpB, ClpA, ClpX  | Desegregation of proteins  | Cytosol and mitochondria                         |

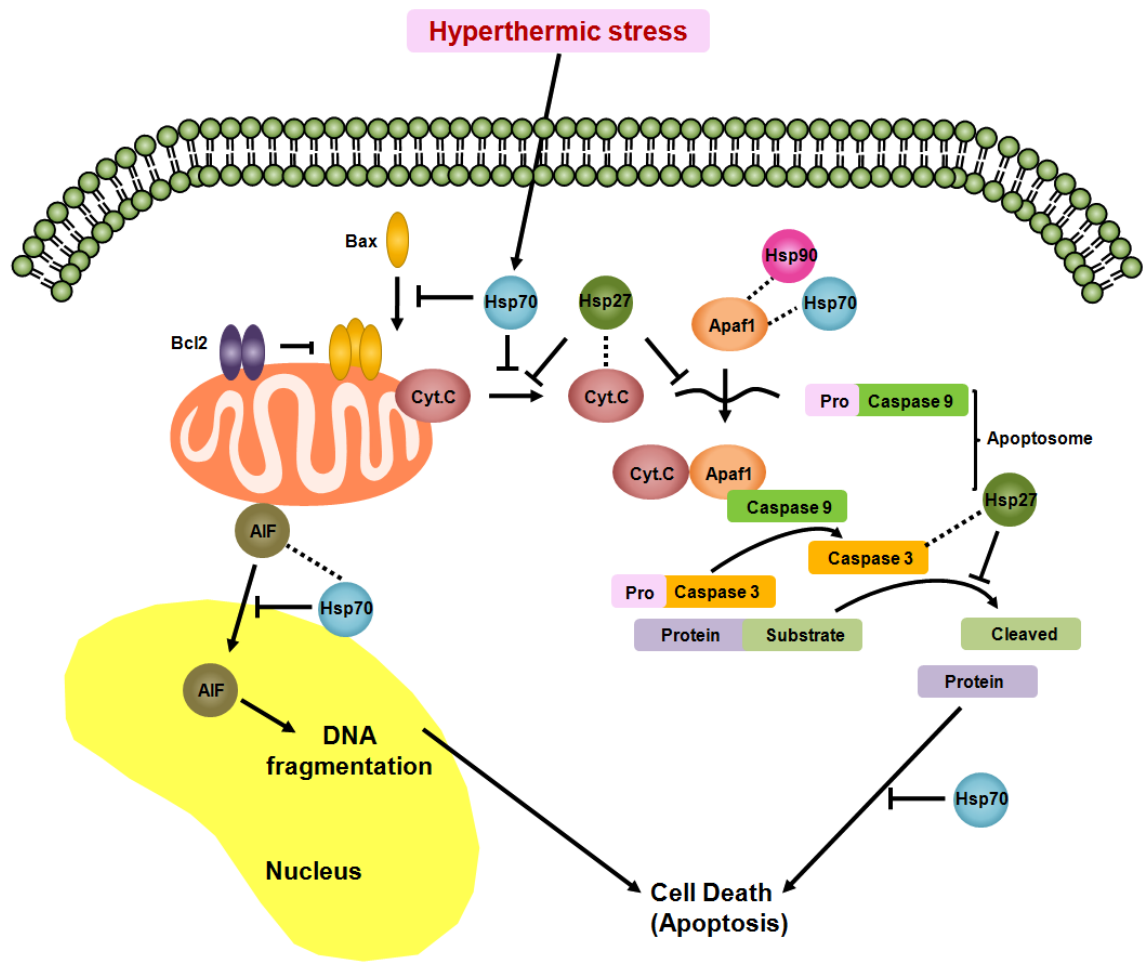


Fig. (1). Schematic illustration for the key role of Hsp groups in suppressing of hyperthermic stress-induced apoptosis [15]. Copyright 2004 Nature Publishing Group.

tochondria; this migration results in the formation of pore that permits release of cytochrome c and apoptosis inducing factor (AIF) [20]. The relationship between Hsp27 and cytochrome c has also been questioned. Although only a very small fraction of the total cytochrome c released from mitochondria is bound to Hsp27, it is unlikely that Hsp27 acts upstream of the apoptosome [21]. However, if Hsp27 is not working, cytochrome c is released from mito-

chondria with dATP and binds to apoptotic protease-activating factor (Apaf1) freed from Hsp90 and Hsp70, which leads to Apaf1 oligomerization and requires the procaspase 9. In turn, apoptosome is formed and apoptosis downstream is executed by activated caspase 9 and caspase 3. The released AIF from mitochondria moves into the nucleus and induces cell death [4].

As mentioned above, the response of cells to a hyperthermic stress relies on its severity, which is influenced by the thermal intensity and duration at high temperature. A transient exposure to elevated temperatures is tolerable because cells are able to turn on the repair mechanism rapidly and respond to the level of protein damage appropriately. However, above a certain threshold, the cell will succumb to a death signaling. Ultimately, the decision to live or die depends on the relative strength of cellular survival and death signals. Therefore, well-designed gold nanostructures (such as nanoshells, nanocages, and nanorods) for the induction of the hyperthermic stress have attracted many scientific endeavors pursuing better cancer treatments without damages for normal tissues [15].

## 2. Photothermal Effect of Gold Nanostructures

Physical-chemical properties of gold nanostructures for photo-induced heat generation by specific light illumination have brightened the prospect of the photo thermal therapy [24-26]. The heat generation process from gold nanostructures involves absorption of photons as well as heat transfer from the nanostructures to the surrounding matrix. In terms of the absorption of photons, gold nanostructures have a strong heating effect because gold is a substance with many free electrons. The free electrons move around from one atom to another but they cannot leave the surface of gold nanostructures. Thus, in the Drude-Lorenz model, gold is regarded as a plasmon [27] because it is composed of equal number of protons which have positive electric charge (fixed in position) and electrons (highly mobile). Under the irradiation of an electromagnetic wave, the free electrons are in rapid oscillations at a plasma frequency and the quantization of plasma oscillation is the plasmon [28]. When gold nanostructures of a finite dimension are exposed to an electromagnetic wave, just the electrons on the surface are the most significant because an electromagnetic wave impinging on the surface of gold nanostructures only has a certain penetration depth. The electric field inside the gold nanostructures shifts the free electrons collectively and then the electrons with negative charge are built up on the surface at one side of gold nanostructure resulting in coherent oscillation in response to the electric field of incident light (Fig. 2) [24, 29, 30]. The free electrons can be collectively displaced from the lattice of positive ions and then, the plasmon is localized to each particle [28]. Their collective oscillations are properly termed as the surface plasmon, and the frequency of irradiated electromagnetic wave corresponds to the surface plasmon wave which leads to a constructive interference and a strong oscillation [27, 29].

This phenomenon leads to the maximum absorbance at the plasmon resonance frequency. Since gold nanostructures are not good light emitters, the total maximum absorbance rate at the plasmon resonance frequency can be converted into the total amount of heat which causes a heat transfer from the gold nanostructures to the environment [31]. Moreover, these photo-induced electrons liberated from gold nanostructures cause the spin and vibrational kinetic energy [32]. During this process, photo-induced electrons are thermalized *via* electron-electron oscillation at the surface of gold nanostructures [33]. Kinetic energy is a general term describ-

ing the energy associated with the motion and thermal energy refers to the kinetic energy of photo-induced electrons. In other words, temperature is a measure of the average kinetic energy of the photo-induced electrons [34]. It is thought that the electron loses its initial linear kinetic energy through collisions with other electrons in the material and then, transfers the energy to the lattice *via* electron-phonon interaction. The last step is the energy transfer to the surrounding matrix [35, 36].

Photothermal cancer therapy using gold nanostructures relies on a surface plasmon resonance red-shifted (650–900 nm) because it is important to reduce absorption by the biological medium [7]. The location and intensity of surface plasmon resonance bands are easily tailored by changing the shape, size and morphology [37-39]. Therefore, controlling the morphology of gold nanostructures is a powerful tool to change the location of maximal absorption wavelength for the photo-induced heat generation. In the next section, we will introduce several forms of gold nanoparticles (gold nanoshells, gold nanorods, hollow gold nanoshells and gold nanoclusters) that achieve a strong absorption at the NIR region.

## 3. Gold Nanostructures for Hyperthermia

Hyperthermia based on gold nanostructures has been greatly publicized as an effective cancer treatment method without side effects [13]. In particular, the use of NIR light is most suitable for photothermal cancer therapy because NIR light can penetrate into the deep tissue due to low absorption from blood and water, and scattering from tissue [40]. In this section, we will discuss various gold nanostructures with a maximal absorption peak at NIR region for photothermal therapy. Optical properties of gold nanostructures can be easily tuned by control of the particle size, shape, composition and structure (Table 3).

### 3.1. Gold Nanoshells

Hirsh *et al.* first demonstrated that gold nanoshells as photothermal agents can be formulated with a dielectric core and a gold shell (Table 3 and Fig. 3a) [47]. Herein, the core is a dielectric material (silica or polymer for example) and the shell is a thin gold layer [48, 49]. Gold nanoshells exhibit similar properties to those of gold nanoparticles and the plasmon resonance of gold nanoshells can be also shifted to the NIR region [50], which is dependent on the relative thickness of gold shell to the core size [51]. The red shift phenomena to NIR region for the effective photothermal cancer therapy can be explained by the plasmon hybridization between inner sphere and outer cavity of gold shell layer [52]. Stern *et al.* studied *in vitro* photothermal therapy using the gold nanoshells against two types of human prostate cancer cell lines. When exposed by NIR light, gold nanoshells can sufficiently raise the surrounding temperature to ablate the cancer cell [53-55]. Loo *et al.* demonstrated the anti-HER2-conjugated gold nanoshells ablate the breast carcinoma cells [39, 56, 57] and silica cored-gold nanoshells as targeted-therapy probe have been applied *in vitro* for glioblastoma [58] and liver cancers [59]. Furthermore, *in vivo* studies have demonstrated the efficacy of gold nanoshells for the non-invasive photothermal therapy [60]. O'Neal *et al.* have successfully treated

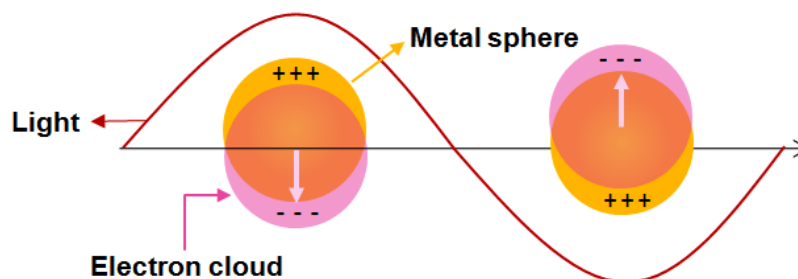
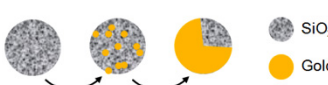
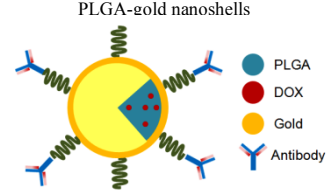
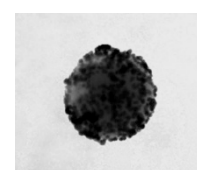
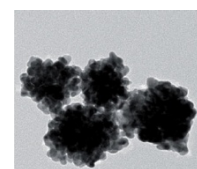
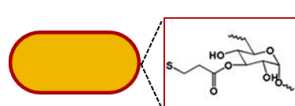
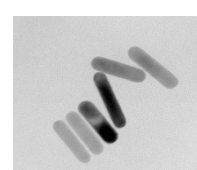
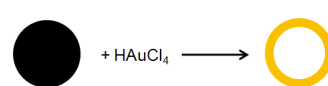
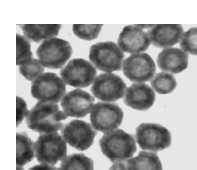
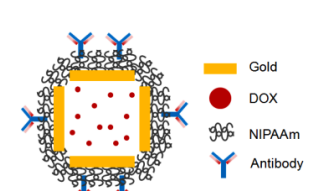
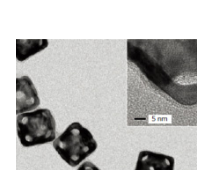
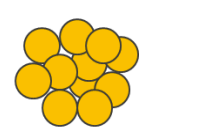
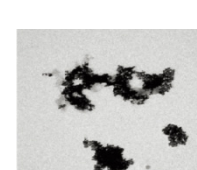


Fig. (2). Schematic illustration of the collective oscillation of free electrons for spherical gold nanostructures.

Table 3. Various Gold-Based Nanoparticles for Photo Thermal Therapy

|         | Scheme  | Morphology  | $\lambda_{\max}$<br>(nm) | Additional             |                                      | Target Disease   | Ref. |
|---------|---|---|--------------------------|------------------------|--------------------------------------|--|------|
|         |   |   |                          | Function               | Agent                                |  |      |
| Shell   | <p>Silica-gold nanoshells</p>  <p>PLGA-gold nanoshells</p>  |   | 840                      | OCT Imaging            |                                      | Breast cancer<br>Prostate Cancer<br>Glioblastoma<br>Liver cancer | [41] |
|         |   |   | 775                      |                        | Targeting moiety<br>Encapsulated DOX | Epithelial Carcinoma   | [42] |
| Rod     |  <p>Gold nanorod<br/>Dextran</p>   |    | 780                      | NIR absorbance imaging | Targeting moiety                     | Inflammation   | [43] |
| Hollow  | <p>Co or Ag nanoparticles + HAuCl<sub>4</sub> →</p>   |   | 628                      |                        | Targeting moiety<br>Encapsulated DOX | Murine Melanomas   | [44] |
|         |  <p>Gold<br/>DOX<br/>NIPAAm<br/>Antibody</p>   |    | 840                      |                        | Targeting moiety<br>Encapsulated DOX | Glioblastoma   | [45] |
| Cluster |  <p>Gold particle</p>  |    | 650                      |                        |                                      | Breast cancer  | [46] |

xenografted mice using gold nanoshells. They showed the gold nanoshell-assisted photothermal ablation would seize the growth of cancer grown in mice and treat allografted tumors in dogs [96]. Especially, gold nanoshells have been studied not only as photothermal therapy agents but also as imaging agents in two photon microscopy and optical coherence tomography [61]. On the other hand, Yang *et al.* introduced the therapeutic system consisting of poly (lactic-co-glycolic acid) (PLGA) core containing doxorubicin (DOX) as a chemotherapeutic agent and a gold over-layer on a polymer matrix capable of a photothermal effect (Fig. 3b) [42].

Gold nanoshells provide advantages for targeted photothermal therapy because light excitation guides local heating. However,

these particles, typically synthesized between 80 and 150 nm in diameter, may be restricted for medical application since this size has problems associated with a quick clearance by the reticulum endothelial system (RES) and a limited diffusion within tissue. Therefore, recent studies tried to overcome these challenges in the size of gold nanoshells.

### 3.2. Gold Nanorods

El-Sayed *et al.* demonstrated the feasibility of gold nanorod-mediated NIR photothermal therapy for the first time in 2005 (Fig. 3a) [62]. Gold nanorods have attracted a particular interest among gold nanostructures because the absorption peak is easily tunable to the NIR region by varying their aspect ratio (length/width) [63, 64].



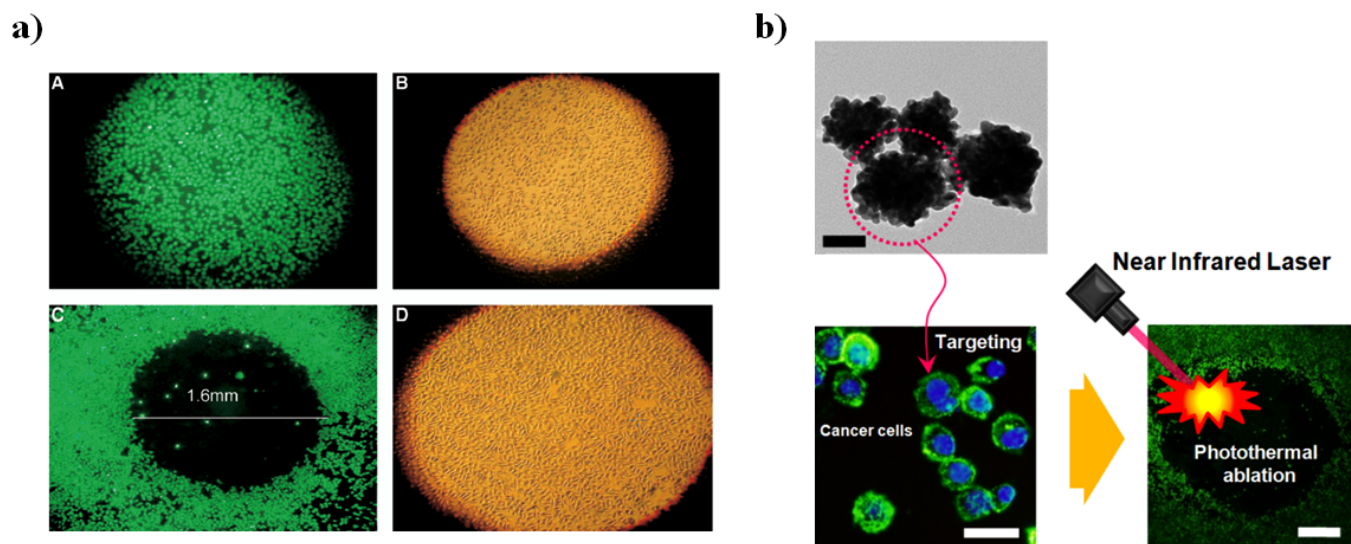


**Fig. (3).** a) Localized photothermal destruction of carcinoma cells using the NIR laser with and without silica gold nanoshells [53] b) Multifunctional drug-loaded PLGA gold nanoshells for multidimensional therapeutic potentials by an NIR laser and DOX as a chemotherapeutic agent [42]. Copyright 2003 American Chemical Society and Copyright 2009 WILEY-VCH Verlag GmbH & Co. KGaA, Weinheim.

Moreover, gold nanorods show additional advantages of small size, high NIR absorption cross section per unit volume, and narrow spectral line widths for photothermal cancer therapy. Owing to their anisotropic shape, the transverse and longitudinal dipole polarizability no longer produces equivalent resonance. Therefore, they have two plasma resonances [65]; the transverse surface plasmon band is located at around 520nm, while the longitudinal surface plasmon band is observed at the near-infrared region. Consequently, gold nanorods are expected to be novel functional materials for analytical, photo functional and biomedical application. In addition, the controllability of the aspect ratio of gold nanorods was found from the study of Murphy *et al.* by varying the amount of silver ions in the seed-mediated growth method [66, 67].

Choi *et al.* synthesized gold nanorods for a targeted delivery and demonstrated the photothermal ablation of target cells under NIR light irradiation. An NIR coherent diode laser (808 nm) was

used to irradiate each well for 5 min using a different laser power density (1.0 and 2.5 W/cm<sup>2</sup>). Calcein AM staining was conducted to classify the live/dead cells, and a strong dark spot was revealed by the combination of targeted gold nanorods and NIR laser at both powers of 1 and 2.5 W/cm<sup>2</sup>. The photothermal experiment using NIR light exhibited a significant cell-killing efficacy, even with a lower concentration of Au and a low-power light source (Fig. 4b) [43].

On the other hand, Dickerson *et al.* presented *in vivo* oncological treatment using gold nanorods in which photon energy is selectively administered and converted into heat sufficient to induce cellular hyperthermia [68]. For *in vivo* application, moreover, the temperature increase is the most important parameter. Chou *et al.* investigated photothermal conversion efficiency by tuning the wavelength to match that of aspect ratio and calculated the ideal temperature rise assuming a 100% photon-to-thermal energy con-

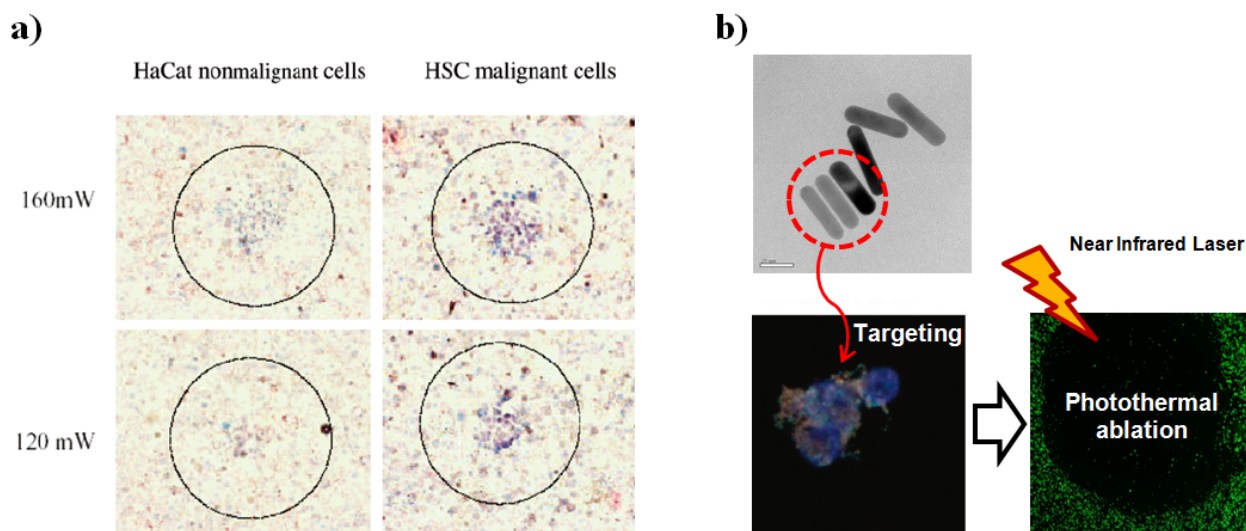


**Fig. (4).** a) Localized photothermal destruction of cancer cells using the NIR laser with gold nanorods under various laser powers [62]. b) Thiolated dextran-coated gold nanorods (DEX-GNRs) synthesis for significant photothermal ablation efficacy at low dose and low laser power and this result supports its use in potential capabilities for the treatment [43]. Copyright 2005 American Chemical Society and Copyright 2010 American Chemical Society.

version, and the heat release process from this volume is much slower than the temperature buildup during the irradiation time [69]. Recent studies showed a comparison of photothermal efficiency between gold nanoshells and nanorods for clinical therapeutic applications [70, 71]. Photothermal conversion efficiency of gold nanorods is superior to that of gold nanoshells. But on the other viewpoint of how much light energy per particle can be converted to heat, gold nanoshells have a significantly larger photothermal transduction cross-section [70]. These distinct characteristics of gold nanorods have provided exciting concepts in the nanomedicine for cancer therapy applications. There are some examples that gold nanorods had also demonstrated *in vivo* therapeutic efficacy against breast cancer, oral squamous carcinoma and colon cancer xenografts by intravenous injection [67, 72].

Similar to other gold nanoparticles, gold nanorods have been studied specifically for their potential as imaging contrast agent with NIR absorbance. Choi *et al.* describe the development of integrin-targeting gold nanorods (cRGD-conjugated gold nanorods), and evaluate their functional use in NIR optical imaging for glioblastoma *in vitro* and *in vivo* [73]. cRGD-conjugated gold nanorods exhibit an excellent tumor-targeting ability with no cytotoxicity. Also, prolonged stability in the blood circulation also contributed to highly efficient cell uptake, internalization and biodistribution (Fig. 5). Therefore, these advantageous features of gold nanorods allowed us to obtain outstanding selective NIR tumor imaging results, demonstrating the utility of this nanoprobe design for future clinical applications.

### 3.3. Hollow Gold Nanoshells

Younan Xia *et al.* demonstrated hollow gold nanoshells for the photothermal therapy. As the name implies, these particles are designed to have a hollow core with 30 nm diameter and a thin gold shell with a thickness of 8 nm [74]. By using galvanic replacement reaction of cobalt [44] and silver [75] with gold, hollow gold nanoshells were produced with tunable sizes and optical properties.

This synthesis utilizes the redox potential between metallic cobalt and silver and gold salt in solution. Cobalt and silver nanoparticles were fabricated and then oxidized by chloroauric acid. At this stage, the core can also be continually oxidized by  $H^+$  and thin shell of gold from  $HAuCl_4$  aqueous solution is created on the surface because the standard reduction potential of the  $H^+/H_2$  redox couple is higher than that of  $Co^{2+}/Co$  and  $Ag^+/Ag$  redox couple [44, 76]. In the study conducted by Li *et al.*, hollow gold nanospheres were attached with a melanocyte-stimulating hormone analog, which targets the melanocortin type-1 receptor over-expressed, and used *in vivo* to ablate tumor [77]. Another type of hollow structure gold nanocages has been developed by Xia *et al.* These particles are formed by simultaneous depletion of silver and deposition of gold, which results in hollow nanostructures with porous walls with an edge length range of 30 to 200 nm. By adjusting the volumes of  $HAuCl_4$  solution, the maximum absorption peak can be varied from 500 nm to 900 nm [78]. Chen *et al.* performed the *in vivo* photothermal efficacy of gold nanocages conjugated with anti-HER2 antibodies using a bilateral tumor model. The gold nanocages served also as a contrast agent in optical coherence tomography [79-81]. In addition, gold nanocages are well suited for drug encapsulation due to hollow and porous structure and for controlled release by NIR light. Furthermore, Chen *et al.* investigated the *in vivo* photothermal efficacy of gold nanocages using a bilateral tumor model [82].

### 3.4. Gold Nanocluster

Gold nanospheres can be prepared by a relatively simple synthetic method and the small size of nanoparticles makes them appealing for photothermal therapy applications. El-Sayed first suggested gold nanospheres for selective photothermal agents against oral squamous carcinoma cell lines *in vitro* using a continuous argon ion laser at 514 nm. They found that the malignant cell could be destroyed with anti-EGFR/gold nanospheres even with four-fold lower laser power compared to one in the absence of gold nano-

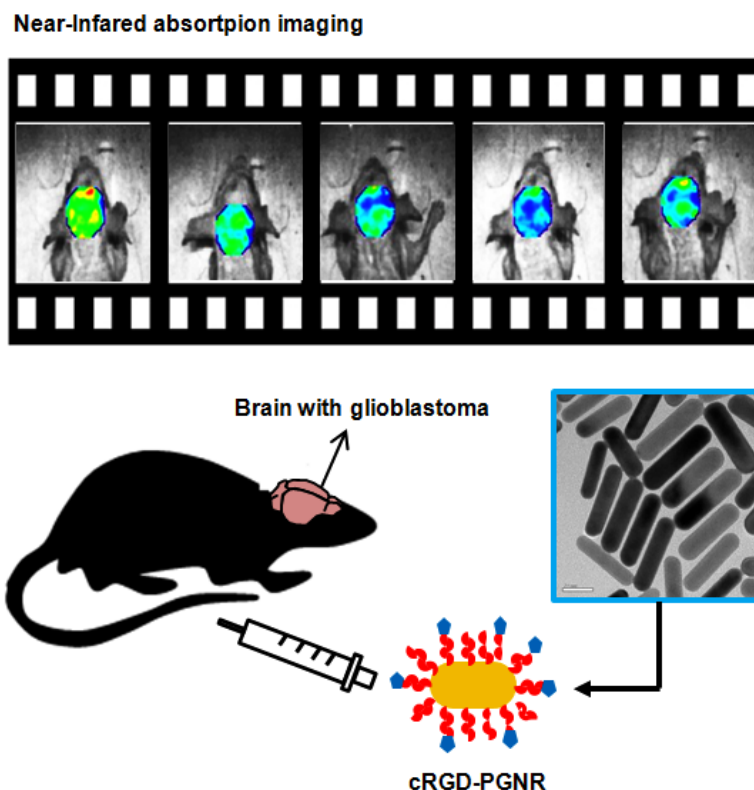


**Fig. (5).** Schematic illustration of the synthesis of cRGD-conjugated gold nanorods as imaging agent that exhibit excellent tumor-targeted imaging ability with no cytotoxicity [73]. Copyright 2009 WILEY-VCH Verlag GmbH & Co. KGaA, Weinheim.

spheres [83]. In the recent work, Li *et al.* reported that gold nanospheres with targeting transfer in molecules can provide imaging and therapy of breast cancer cell line using a nanosecond laser operating at 530 nm. As a result, transfer in conjugated gold nanospheres bound to Hs578T cells with a six-fold higher affinity that of control group exhibited two-fold higher photothermal efficiency [84].

Despite the success in using gold nanospheres for *in vitro*, these particles have a limitation for *in vivo* application owing to maximum absorbance peak in the visible region at the around 500 nm. Aggregated gold nanospheres show a similar behavior to gold nanorods because aggregated gold nanospheres cause a coupling of plasmon modes, which results in a red shift and broadening of the longitudinal plasmon resonance [46, 85]. Being conjugated to anti-epidermal growth factor receptor (anti-EGFR) antibodies, gold nanospheres bind specifically to the HSC 3 cancer cells. Under exposure to a femtosecond NIR laser, a twenty-fold lower laser power could destroy cancer cells [82]. Nam *et al.* demonstrated that gold nanospheres can be deliberately designed to aggregate in mildly acidic conditions. The pH-induced aggregation of gold nanospheres led to absorption in the NIR, which could be exploited for a photothermal cancer therapy [46].

#### 4. Targeted Delivery of Gold Nanostructures

Rapid clearance of nanoparticles from the blood after the intravenous injection is the main reason of failure for nanoparticle-based therapy. In order to circumvent the RES intake, various parameters such as nanoparticle size and surface-moieties have been studied [86, 87]. Jong *et al.* found that the biodistribution of gold nanospheres is size-dependent. Various sized gold nanospheres (10, 50, 100 and 250 nm) were intravenously injected into the rat, and the gold components in the organs including blood, heart, lung, liver, spleen, kidney thymus, brain and testis were measured by using ICP-MS. As a result, the smallest particles showed the most widespread tissue distribution and relatively higher concentration of gold compared to larger particles (Table 4) [88]. Similarly, Terentyuk *et al.* evaluated the particle-size effects on the distribution of 15 nm, 50 nm of PEGylated gold nanospheres and 160 nm of silica/gold nanoshells in rat and rabbit, respectively. As expected, the smallest 15 nm particles were widely distributed among the entire organs, while 160 nm gold nanoshells were accumulated mainly in the liver and spleen [89]. Other types of surface modification have been suggested for biomedical applications. Other types of surface modification have been suggested for biomedical applications. Atsushi *et al.* showed the gold nanorods were coated with thermoresponsive polymers such as *N,N*-dimethylacrylamide (DMAA) or acrylamide (AAM) to *N*-isopropylacrylamide (NIPAM) which have different phase transition temperature. Irradiation using the near-infrared laser induced a decreased in their sizes. Among them,

Poly(NIPAM-AAm)-coated gold nanorods have stable circulation time without a phase transition and specifically accumulating in the tumor [90]. Choi *et al.* showed thiolated dextran-coated gold nanorods for efficient targeted delivery and low cytotoxicity in comparison to hexadecyltrimethylammonium bromide (CTAB)-coated gold nanorods [43] and Kim *et al.* demonstrated that CTAB was successfully replaced with PCL dish and Pluronic F127 that enhanced the biocompatibility and extended to drug delivery system because of the presence of PCL, which is available as a drug delivery vehicle [91].

Furthermore, the surface of gold nanostructures has been mostly modified with polyethylene glycol (PEG) for enhanced non-fouling effects. Gold nanostructures modified with PEG as a surface brush layer exhibit a protein resistance and non-immunogenicity, because the segmental flexibility produces a high degree of steric exclusion and reduces the entropy at interfaces between PEG and water molecules [92]. Therefore, the blood half-life of gold nanostructures can be greatly extended. Perrault *et al.* evaluated the effect of PEG molecular weight having final hydrodynamic diameters of approximately 20, 40, 60, 80, and 100 nm. As shown in Fig. (6), the circulation time of gold nanostructures is improved with smaller particle diameter and larger PEG molecular weight [93].

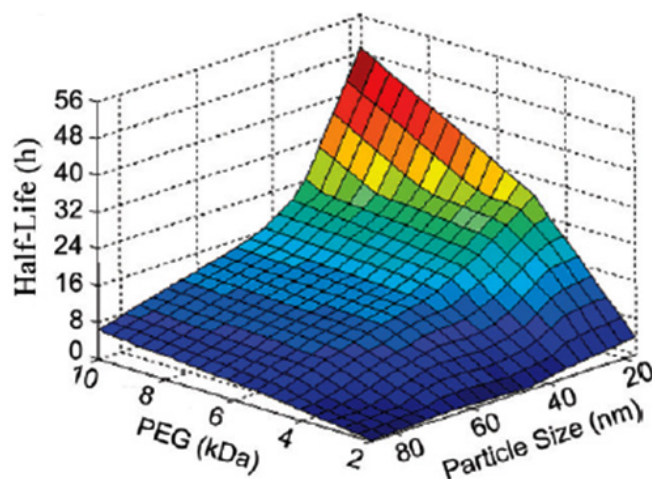


Fig. (6). Effect of PEG molecular weight and particle size of gold nanoparticles on the blood half-life [92]. Copyright 2009 American Chemical Society.

Recently, Jiang *et al.* demonstrated that 25-50 nm gold nanostructures conjugated with targeting moieties have a long blood half-

Table 4. Biodistribution of the Average Number of Gold Particles to the Various Organs. Copyright 2008 Elsevier

| Organs | Number of Particles/ Mass of Organ |          |          |          |
|--------|------------------------------------|----------|----------|----------|
|        | 10 nm,                             | 50 nm    | 100 nm   | 250 nm   |
| Blood  | 1.9E+ 12                           | 1.2E+ 10 | 2.2E+ 09 | 4.6E+ 07 |
| Liver  | 2.4E+ 12                           | 8.2E+ 09 | 2.3E+ 09 | 9.5E+ 07 |
| Spleen | 1.1E+ 11                           | 5.2E+ 08 | 7.3E+ 07 | 3.8E+ 06 |
| Lung   | 1.4E+ 10                           | 9.0E+08  | 2.2E+ 06 | 1.2E+ 05 |
| Kidney | 4.9E+ 10                           | 6.5E+ 07 | 3.8E+ 06 | 1.6E+ 05 |
| Testis | 1.1E+ 10                           | —        | —        | 4.2E+ 04 |
| Thymus | 9.1E+ 09                           | —        | —        | 6.4E+ 04 |
| Heart  | 9.9E+ 09                           | 2.2E+07  | 4.3E+ 05 | —        |
| Brain  | 1.6E+10                            | —        | —        | —        |



life and are also in the optimal size range for a cellular uptake *in vitro* and for a broad biodistribution of gold nanostructures in a tumor mass (Fig. 7a) [94], which are very important to increase the therapeutic effectiveness. Fluid pressure in a tumor mass is high in the center and low in the periphery and surrounding tissue. Therefore, gold nanostructures that enter the tumor through leaky vasculature migrate to the tumor periphery and into the surrounding tissue [93, 94]. Moreover, Perrault *et al.* demonstrated the washout time and intra-tumoral distribution depended on the size of gold nanostructures and observed that permeation into the tumor decreased with increasing nanoparticle size (Fig. 7b) [93].

In conclusion, the selection of gold nanostructures with an appropriate maximum absorption wavelength and a surface chemistry is essential to improve gold nanoparticle tumor accumulation and retention. Furthermore, the photothermal cancer therapy using gold nanostructures should be considered along with the choice of the light-irradiating modality, which will be described in the following section.

### 5. Method to Provide Irradiating Energy

In general, the NIR light is useful for *in vivo* photothermal therapy application because hemoglobins and water molecules, the

major absorbers of visible and infrared light, have their lowest absorption coefficient in the NIR region; the absorption coefficient is as much as two orders of magnitude smaller in the NIR region (650–900 nm) as compared to the visible region (400–600 nm). Thus, the NIR light can penetrate much deeper into tissue than the visible light [40, 97]. One of the most promising approaches is utilizing gold nanostructure-mediated photothermal therapy to operate in the “NIR window” to minimize attenuation of the light caused by unnecessary light-tissue interactions and to avoid damages in a healthy tissue. It has been shown that photon excitation of surface plasmon bands generates excited states in the free electrons on the surface of the gold nanoparticle; phonons are then released after relaxation of the electrons. The phonons subsequently relax and are converted to heat within 100 ps [35, 36]. Consequently, most photons absorbed by gold nanostructures are transformed into heat.

Various laser types, such as continuous-wave laser, pulsed-mode laser or dual laser, had been suggested for enhanced NIR therapy. Many types of lasers can be made to operate in a continuous wave mode to satisfy as the requirement of a photothermal therapy application. For example, El-Sayed *et al.* demonstrated that anti-EGFR antibody-conjugated gold nanorods cause photothermal destruction by near-infrared continuous-wave laser at 800 nm [47,

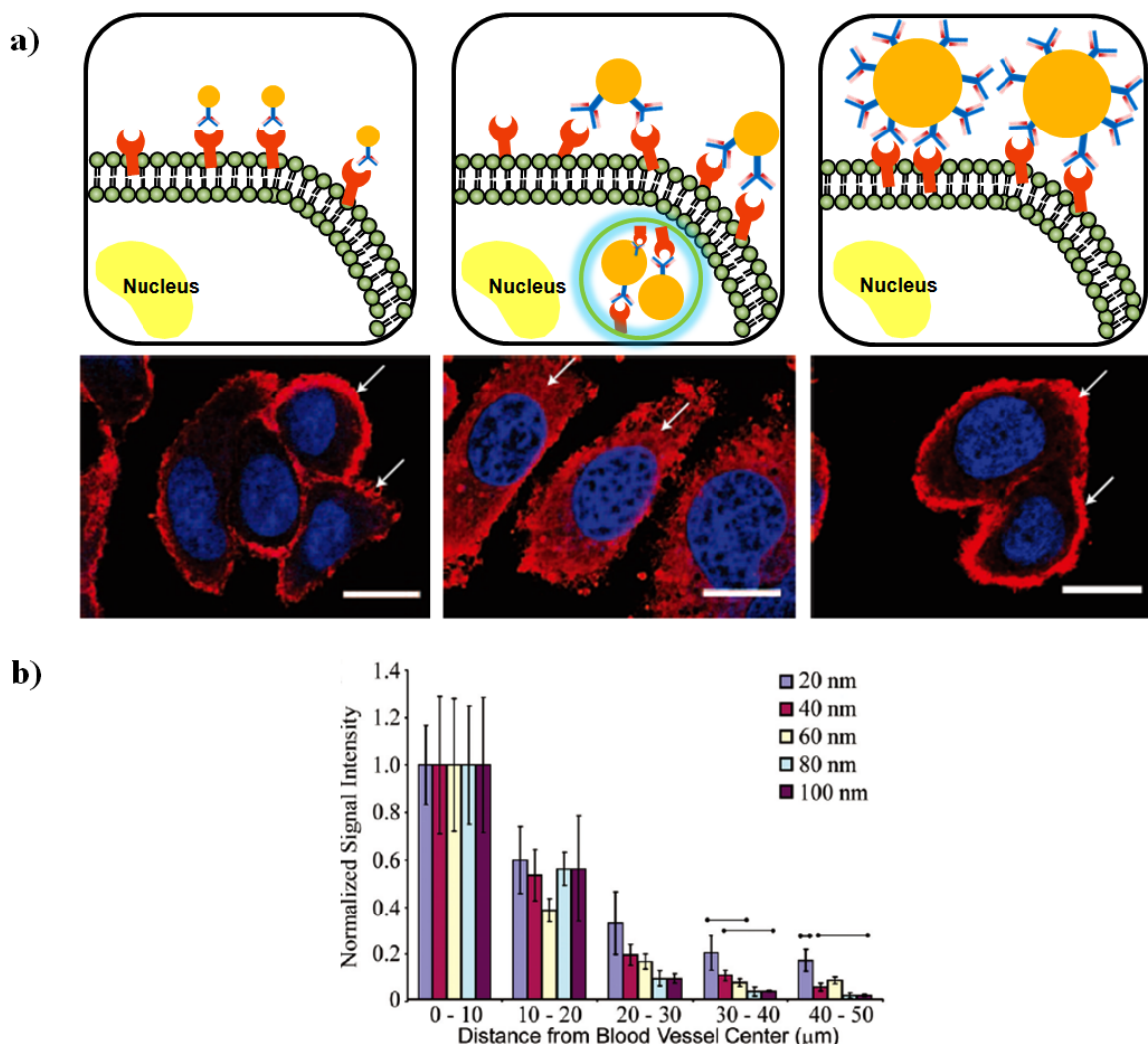


**Fig. (7).** **a)** Illustrations with corresponding fluorescence images of Her2/neureceptor localization after treatment with different-sized Herceptin-conjugated gold nanostructures. Arrows indicate Her2/neureceptors, and the nucleus is counterstained with DAPI (blue) [94]. Copyright 2008 Nature Publishing Group. **b)** Gold nanostructures distribution with respect to distance from tumor blood vessels by densitometry analysis of tumor section [93]. Copyright 2009 American Chemical Society.



58, 62]. In a recent study, however, one alternative is the use of a pulsed-mode laser instead of a continuous-wave laser. Since the pulse energy is equal to the average power divided by the retention rate, enough laser power can be obtained by lowering the rate of pulsed so that more energy can be built up in between pulses. In particular, pulsed laser for the photothermal ablation of cancer cells permits more efficient photothermal conversion, because lapses between the pulses allow an additional time for electron-phonon relaxation. Table 5 indicates that pulsed-mode lasers are more efficient to induce cell damages than continuous-wave lasers; the ab-

sorbance of gold nanostructures is saturated under continuous-wave laser, thus decreasing the absorbance efficiency and the overall energy conversion. Therefore, pulsed-mode laser is desirable for cancer treatment. Folate-conjugated gold nanorods can be targeted to tumor cells for photo-induced injury using NIR irradiation [11]. Membrane blebbing was observed after exposure to a femtosecond-pulsed NIR laser at a power as low as 0.75 mW *in vitro*, whereas a continuous-wave laser required a power of 6 mW to achieve the same effect (Fig. 8) [11]. When a tumor in the early stage was exposed to a single laser for therapy, an undesirable overheating could

**Table 5.** Energy Thresholds for Various Shapes of Gold Nanostructures for Photothermal Cancer Therapy. Copyright 2010 IEEE

| Laser Mode | Shape  | Unit | Laser Source | Wavelength (nm) | Repetition Rate (MHz) | Energy Threshold (mJ/cm <sup>2</sup> ) | Ref.  |
|------------|--------|------|--------------|-----------------|-----------------------|--|-------|
| CW         | Shell  |      |              | 820             |                       | $3.4 \times 10^7$                      | [57]  |
|            | Rod    |      | Ti:sapphire  | 800             |                       | $2.4 \times 10^6$                      | [62]  |
|            | Sphere |      | Argon        |                 |                       | $2.4 \times 10^3$                      | [11]  |
| Pulsed     | Shell  | Fs   |              | 800             |                       | $1.6 \times 10^3$                      | [49]  |
|            | Rod    | Fs   | Ti:sapphire  | 800             | 80                    | 15.8 (linear pl)                       | [101] |
|            |        |      |              | 765             |                       | 7.9 (circular pl)                      |       |
|            | Sphere | Fs   | Ti:sapphire  | 800             |                       | $2.1 \times 10^5$                      | [102] |
|            |        | ns   |              | 530             | 10                    | $2.1 \times 10^6$                      | [84]  |

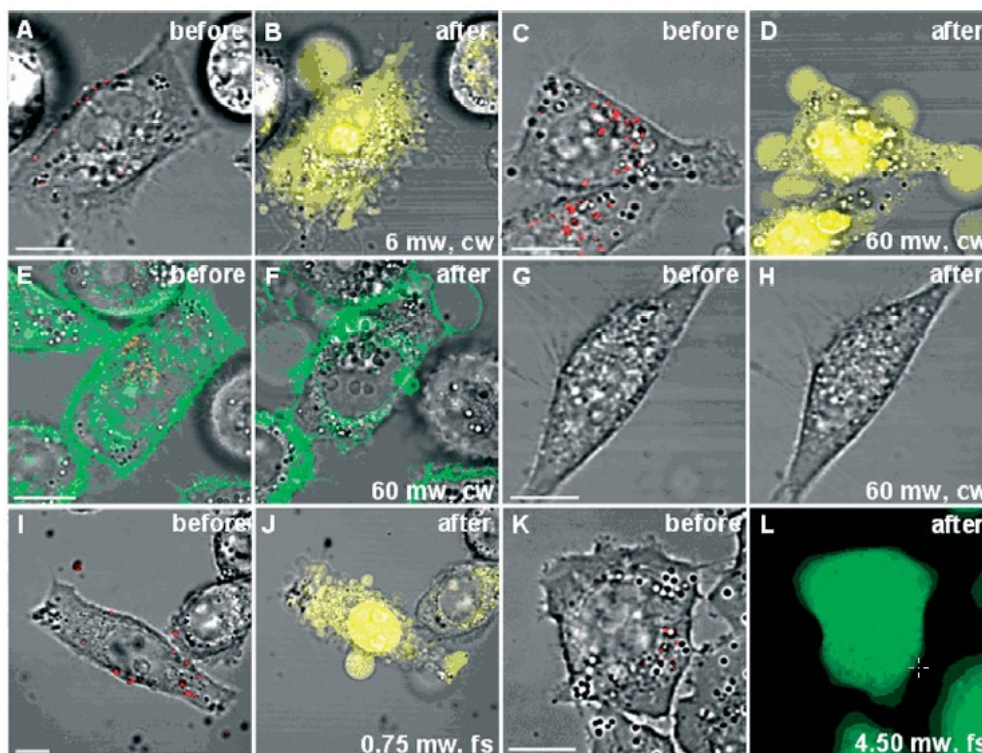


**Fig. (8).** Site-dependent photothermolysis mediated by folate-conjugated gold nanorods (red). (A,B) Cells with membrane-bound folate-conjugated gold nanorods exposed to CW NIR laser irradiation experienced membrane perforation and blebbing at 6 mW. The loss of membrane integrity was indicated by EB staining (yellow). (C,D) Cells with internalized F-NRs required 60 mW to produce a similar level of response. (E,F) folate-conjugated gold nanorods internalized in KB cells labeled by folate-Bodipy (green) were exposed to laser irradiation at 60 mW, resulting in both membrane blebbing and disappearance of the folate-conjugated gold nanorods. (G,H) NIH-3T3 cells were unresponsive to folate-conjugated gold nanorods, and did not suffer photo-induced damage upon 60 mW laser irradiation. (I,J) Cells with membrane-bound folate-conjugated gold nanorods exposed to fs-pulsed laser irradiation produced membrane blebbing at 0.75 mW. (K,L) Cells with internalized folate-conjugated gold nanorods remained viable after fs-pulsed irradiation at 4.50 mW, as indicated by a strong calcein signal (green) [11]. Copyright 2007 WILEY-VCH Verlag GmbH & Co. KGaA, Weinheim.

occur. It was proposed that this uneven heating could be alleviated by the use of a dual-laser heating configuration such as a fiber-optic probe within the tumor to conduct NIR light, which would eventually lead to a minimally invasive therapy [98]. Schwartz *et al.* practiced nanoshell-mediated therapy for tumors in the brain using a fiber-optic probe [98]. On the other hand, exact simulation of the thermal profile effect of nanoparticle-loaded tissue is essential to achieve a maximal heat ablation in real solid tumors [70, 99]. Vera *et al.* investigated the effects of gold nanoshells distribution density, laser power intensity, and laser arrangement on the induced heat for five different tissue types [100]. Maltzahn *et al.* computationally demonstrated a photothermal tumor therapy using gold nanoparticles and compared photothermal efficacy of gold nanorods with that of gold nanoshells [99].

## CONCLUSION

In recent years, NIR-absorbing gold nanostructures such as gold nanoshells, gold nanorods, gold nanocages and aggregated gold nanoparticles have come into the spotlight as photothermal agents due to the potential for *in vivo* cancer ablation. In particular, the tuning of surface plasmon resonance bands for gold nanostructure from the visible region to the near infrared region makes them ideal for a photothermal cancer therapy and imaging. For the efficient cancer treatment, however, we should have a better understanding of the intrinsic properties of gold nanostructures by further controlling the shape, size and surface modification. In this review, we presented i) the mechanism for the cellular death signaling induced by a thermal stress, ii) the overview on the fundamental properties of gold nanostructures for the photothermal ablation and imaging of cancer cells, iii) various gold nanostructure designs to have a maximum absorption band at the NIR region and iv) therapy optimization strategies involving nanoparticle surface modification and laser operation method for an enhanced accumulation of gold nanostructures to the target cancer and for an effective cancer cell ablation. With further developments in this research field in a timely manner, these advantageous features of gold nanostructures as theragnostic agents would soon allow us to greatly improve the quality of life for cancer patients.

## ACKNOWLEDGEMENTS

This work was supported by National Research Foundation grant funded by the Korea government (MEST) (No.2010-0020648) and by a grant of the Korea Healthcare technology R&D Project, Ministry for Health, Welfare & Family Affairs, Republic of Korea (A090728). This study was supported by a grant of the Korea Health 21 R&D Project, Ministry of Health & Welfare, Republic of Korea (A101954).

## REFERENCE

- [1] I. Bland, K.; Daly, J.M.; P. Karakousis, C. Surgical Oncology. *McGraw-Hill Professional*, **2001**, 1221-23.
- [2] Markman, M.; Reichman, B.; Hakes, T.; Curtin, J.; Jones, W.; Lewis, J.L.; Barakat, R.; Rubin, S.; Mychalczak, B.; Saigo, P.; Almadrones, L.; Hoskins, W. Intraperitoneal chemotherapy in the management of ovarian cancer. *Cancer*, **1993**, *71*, 1565-70.
- [3] Fu, K.K.; Pajak, T.F.; Trotti, A.; Jones, C.U.; Spencer, S.A.; Phillips, T.L.; Garden, A.S.; Ridge, J.A.; Cooper, J.S.; Ang, K.K. A radiation therapy oncology group (RTOG) phase III randomized study to compare hyperfractionation and two variants of accelerated fractionation to standard fractionation radiotherapy for head and neck squamous cell carcinomas: first report of RTOG 9003. *Int. J. Radiat. Oncol. Biol. Phys.*, **2000**, *48*, 7-16.
- [4] Fu, K.; Phillips, T.; Silverberg, I.; Jacobs, C.; Goffinet, D.; Chun, C.; Friedman, M.; Kohler, M.; McWhirter, K.; Carter, S. Combined radiotherapy and chemotherapy with bleomycin and methotrexate for advanced inoperable head and neck cancer: update of a Northern California Oncology Group randomized trial. *J. Clin. Oncol.*, **1987**, *5*, 1410-18.
- [5] Hesketh, P.J. Chemotherapy-Induced Nausea and Vomiting. *N. Engl. J. Med.*, **2008**, *358*, 2482-94.
- [6] Crawford, J.; Ozer, H.; Stoller, R.; Johnson, D.; Lyman, G.; Tabbara, I.; Kris, M.; Grous, J.; Picozzi, V.; Rausch, G.; Smith, R.; Gradishar, W.; Yahanda, A.; Vincent, M.; Stewart, M.; Glaspy, J. Reduction by Granulocyte Colony-Stimulating Factor of Fever and Neutropenia Induced by Chemotherapy in Patients with Small-Cell Lung Cancer. *N. Engl. J. Med.*, **1991**, *325*, 164-70.
- [7] Dees, C.; Harkins, J.; Petersen, M.G.; Fisher, W.G.; Wachter, E.A. Treatment of Murine Cutaneous Melanoma with Near Infrared Light. *Photochem. Photobiol.*, **2002**, *75*, 296-301.
- [8] Goodrich, G.P.; Bao, L.; Gill-Sharp, K.; Sang, K.L.; Wang, J.; Payne, J.D. Photothermal therapy in a murine colon cancer model using near-infrared absorbing gold nanorods. *J. Biomed. Opt.*, **2010**, *15*, 018001.
- [9] Lee, S.-M.; Park, H.; Yoo, K.-H. Synergistic Cancer Therapeutic Effects of Locally Delivered Drug and Heat Using Multifunctional Nanoparticles. *Adv. Mater.*, **2010**, *22*, 4049-53.
- [10] Gobin, A.M.; Watkins, E.M.; Quevedo, E.; Colvin, V.L.; West, J.L. Near-Infrared-Resonant Gold/Gold Sulfide Nanoparticles as a Photothermal Cancer Therapeutic Agent. *Small*, **2010**, *6*, 745-52.
- [11] Tong, L.; Zhao, Y.; Huff, T.B.; Hansen, M.N.; Wei, A.; Cheng, J.X. Gold Nanorods Mediate Tumor Cell Death by Compromising Membrane Integrity. *Adv. Mater.*, **2007**, *19*, 3136-41.
- [12] Boyce, M.; Yuan, J. Cellular response to endoplasmic reticulum stress: a matter of life or death. *Cell. Death. Differ.*, **2006**, *13*, 363-73.
- [13] Shellman, Y.G.; Howe, W.R.; Miller, L.A.; Goldstein, N.B.; Pacheco, T.R.; Mahajan, R.L.; LaRue, S.M.; Norris, D.A. Norris. Hyperthermia Induces Endoplasmic Reticulum-Mediated Apoptosis in Melanoma and Non-Melanoma Skin Cancer Cells. *J. Invest. Dermatol.*, **2007**, *128*, 949-56.
- [14] Aitken, R.J.; Gordon, E.; Harkiss, D.; Twigg, J.P.; Milne, P.; Jennings, Z.; Irvine, D.S. Relative Impact of Oxidative Stress on the Functional Competence and Genomic Integrity of Human Spermatozoa. *Biol. Reprod.*, **1998**, *59*, 1037-46.
- [15] Mosser, D.D.; Morimoto, R.I. Molecular chaperones and the stress of oncogenesis. *Oncogene*, **2004**, *23*, 2907-18.
- [16] Fulda, S.; Gorman, A.M.; Hori, O.; Samali, A. Samali. Cellular Stress Responses: Cell Survival and Cell Death. *International Journal of Cell Biology*, **2010**, *2010*, 23.
- [17] Hartl, F.U.; Hayer-Hartl, M. Molecular Chaperones in the Cytosol: from Nascent Chain to Folded Protein. *Science*, **2002**, *295*, 1852-58.
- [18] C.Freeman, B.; I.Morimoto, R. The human cytosolic molecular chaperones hsp90, hsp70 (hsc70) and hdi-1 have distinct roles in recognition of a non-native protein and protein refolding. *EMBO J.*, **1996**, *15*, 2969-79.
- [19] M, H.; J., B. Chaperone function of sHsps. *Progress in molecular and subcellular biology*, **2002**, *28*, 37-59.
- [20] Jürgensmeier, J.M.; Xie, Z.; Deveraux, Q.; Ellerby, L.; Bredesen, D.; Reed, J.C. Bax directly induces release of cytochrome c from isolated mitochondria. *Proceedings of the National Academy of Sciences*, **1998**, *95*, 4997-5002.
- [21] Paul, C.; Manero, F.; Gonin, S.; Kretz-Remy, C.; Viot, S.; Arrigo, A.-P. Hsp27 as a Negative Regulator of Cytochrome c Release. *Mol. Cell. Biol.*, **2002**, *22*, 816-34.
- [22] Benjamin, I.J.; McMillan, D.R. Stress (Heat Shock) Proteins : Molecular Chaperones in Cardiovascular Biology and Disease. *Circ. Res.*, **1998**, *83*, 117-32.
- [23] Schlesinger, M.J. Heat shock proteins. *J. Biol. Chem.*, **1990**, *265*, 12111-14.
- [24] Liu, M.; Guyot-Sionnest, P.; Lee, T.-W.; Gray, S.K. Optical properties of rodlike and bipyramidal gold nanoparticles from three-dimensional computations. *Phys. Rev. B.*, **2007**, *76*, 235428.
- [25] Bohren, C.F.; Huffman, D.R. Absorption and Scattering of Light by Small Particles. *John Wiley & Sons*, **1998**, 1-544.
- [26] Kreibitz, U.; Vollmer, M. Optical Properties of Metal Clusters. *Springer Series in Materials Science*, **1995**.
- [27] Kittel, C. Introduction to solid state physics. *6th, John Wiley & Sons*, **1986**.
- [28] Johnson, W.L. Shape-controlled synthesis and surface plasmonic properties of metallic nanostructures. *MRS Bull.*, **2005**, *30*, 338-48.

- [29] Hutter, E.; Fendler, J.H. Exploitation of Localized Surface Plasmon Resonance. *Adv. Mater.*, **2004**, *16*, 1685-706.
- [30] Link, S.; El-Sayed, M.A. Shape and size dependence of radiative, non-radiative and photothermal properties of gold nanocrystals. *Int. Rev. Phys. Chem.*, **2000**, *19*, 409 - 53.
- [31] Govorov, A.O.; Richardson, H.H. Generating heat with metal nanoparticles. *Nano Today*, **2007**, *2*, 30-38.
- [32] Sears, F.W.; Zemansky, M.W.; Young, H.D. University Physics, Sixth Edition. *Addison-Wesley*, **1983**, 843-4.
- [33] Mohamed, M.B.; Ahmadi, T.S.; Link, S.; Braun, M.; El-Sayed, M.A. Hot electron and phonon dynamics of gold nanoparticles embedded in a gel matrix. *Chem. Phys. Lett.*, **2001**, *343*, 55-63.
- [34] Spitzer, L., Jr. The Temperature of Interstellar Matter. *Astrophys. J.*, **1947**, *107*, 6-33.
- [35] Eesley, G.L. Observation of Nonequilibrium Electron Heating in Copper. *Phys. Rev. Lett.*, **1983**, *51*, 2140.
- [36] Eesley, G.L. Generation of nonequilibrium electron and lattice temperatures in copper by picosecond laser pulses. *Phys. Rev. B.*, **1986**, *33*, 2144.
- [37] Lee, K.-S.; El-Sayed, M.A. El-Sayed. Dependence of the Enhanced Optical Scattering Efficiency Relative to That of Absorption for Gold Metal Nanorods on Aspect Ratio, Size, End-Cap Shape, and Medium Refractive Index. *J. Phys. Chem. B*, **2005**, *109*, 20331-38.
- [38] Kang, J.; Yang, J.; Lee, J.; Oh, S.J.; Moon, S.; Lee, H.J.; Lee, S.C.; Son, J.-H.; Kim, D.; Lee, K.; Suh, J.-S.; Huh, Y.-M.; Haam, S. Gold-layered calcium phosphate plasmonic resonants for localized photothermal treatment of human epithelial cancer. *J. Mater. Chem.*, **2009**, *19*, 2902-05.
- [39] Loo, C.; Lin, A.; Hirsch, L.; Lee, M.-H.; Barton, J.; Halas, N.; West, J.; Drezek, R. Nanoshell-enabled photonics-based imaging and therapy of cancer. *Technology in Technol. Cancer Res. Treat.*, **2004**, *3*, 33-40.
- [40] Weissleder, R. A clearer vision for *in vivo* imaging. *Nat. Biotech.*, **2001**, *19*, 316-17.
- [41] Kah, J.C.Y.; Chow, T.H.; Ng, B.K.; Razul, S.G.; Olivo, M.; Sheppard, C.J.R. Sheppard. Concentration dependence of gold nanoshells on the enhancement of optical coherence tomography images: a quantitative study. *Appl. Opt.*, **2009**, *48*, D96-D108.
- [42] Yang, J.; Lee, J.; Kang, J.; Oh, S.J.; Ko, H.-J.; Son, J.-H.; Lee, K.; Suh, J.-S.; Huh, Y.-M.; Haam, S. Smart Drug-Loaded Polymer Gold Nanoshells for Systemic and Localized Therapy of Human Epithelial Cancer. *Adv. Mater.*, **2009**, *21*, 4339-42.
- [43] Choi, R.; Yang, J.; Choi, J.; Lim, E.-K.; Kim, E.; Suh, J.-S.; Huh, Y.-M.; Haam, S. Thiolated Dextran-Coated Gold Nanorods for Photothermal Ablation of Inflammatory Macrophages. *Langmuir*, **2010**, *26*, 17520-27.
- [44] Liang, H.-P.; Wan, L.-J.; Bai, C.-L.; Jiang, L. Gold Hollow Nanospheres: Tunable Surface Plasmon Resonance Controlled by Interior-Cavity Sizes. *J. Phys. Chem. B*, **2005**, *109*, 7795-800.
- [45] Yavuz, M.S.; Cheng, Y.; Chen, J.; Cobley, C.M.; Zhang, Q.; Rycenga, M.; Xie, J.; Kim, C.; Song, K.H.; Schwartz, A.G.; Wang, L.V.; Xia, Y. Gold nanocages covered by smart polymers for controlled release with near-infrared light. *Nat. Mater.*, **2009**, *8*, 935-39.
- [46] Nam Nam, J.; Won, N.; Jin, H.; Chung, H.; Kim, S. pH-Induced Aggregation of Gold Nanoparticles for Photothermal Cancer Therapy. *J. Am. Chem. Soc.*, **2009**, *131*, 13639-45.
- [47] Hirsch, L.R.; Stafford, R.J.; Bankson, J.A.; Sershen, S.R.; Rivera, B.; Price, R.E.; Hazle, J.D.; Halas, N.J.; West, J.L. Nanoshell-mediated near-infrared thermal therapy of tumors under magnetic resonance guidance. *Proc. Natl. Acad. Sci. U. S. A.*, **2003**, *100*, 13549-54.
- [48] Rasch, M.R.; Sokolov, K.V.; Korgel, B.A. Limitations on the Optical Tunability of Small Diameter Gold Nanoshells. *Langmuir*, **2009**, *25*, 11777-85.
- [49] Kim, J.; Park, S.; Lee, J.E.; Jin, S.M.; Lee, J.H.; Lee, I.S.; Yang, I.; Kim, J.-S.; Kim, S.K.; Cho, M.-H.; Hyeon, T. Hyeon. Designed Fabrication of Multifunctional Magnetic Gold Nanoshells and Their Application to Magnetic Resonance Imaging and Photothermal Therapy. *Angew. Chem.-Int. Edit.*, **2006**, *45*, 7754-58.
- [50] Jain, P.K.; Lee, K.S.; El-Sayed, I.H.; El-Sayed, M.A. Calculated Absorption and Scattering Properties of Gold Nanoparticles of Different Size, Shape, and Composition: Applications in Biological Imaging and Biomedicine. *J. Phys. Chem. B*, **2006**, *110*, 7238-48.
- [51] Khlebtsov, B.; Zharov, V.; Melnikov, A.; Tuchin V. *et al.*, Optical amplification of photothermal therapy with gold nanoparticles and nanoclusters. *Nanotechnology*, **2006**, *17*, 5167.
- [52] Prodan, E.; Radloff, C.; Halas, N.J.; Nordlander, P. A Hybridization Model for the Plasmon Response of Complex Nanostructures. *Science*, **2003**, *302*, 419-22.
- [53] Stern, J.M.; Cadeddu, J.A. Emerging use of nanoparticles for the therapeutic ablation of urologic malignancies. *Urol. Oncol.-Semin. Orig. Investig.*, **2008**, *26*, 93-96.
- [54] Gobin, A.M.; Moon, J.J.; West, J.L. EphrinA1-targeted nanoshells for photothermal ablation of prostate cancer cells. *Int. J. Nanomed.*, **2008**, *3*, 351-58.
- [55] Stern, J.M.; Stanfield, J.; Lotan, Y.; Park, S.; Hsieh, J.-T.; Cadeddu, J.A. Efficacy of laser-activated gold nanoshells in ablating prostate cancer cells *in vitro*. *Journal of endourology Endourological Society*, **2007**, *21*, 939-43.
- [56] Loo, C.; Lowery, A.; Halas, N.; West, J.; Drezek, R. Drezek. Immunotargeted Nanoshells for Integrated Cancer Imaging and Therapy. *Nano. Letters.*, **2005**, *5*, 709-11.
- [57] Loo, C.; Hirsch, L.; Lee, M.-H.; Chang, E.; West, J.; Halas, N.; Drezek, R. Gold nanoshell bioconjugates for molecular imaging in living cells. *Opt. Lett.*, **2005**, *30*, 1012-14.
- [58] Bernardi, R.; Lowery, A.; Thompson, P.; Blaney, S.; West, J. Immunonanoshells for targeted photothermal ablation in medulloblastoma and glioma: an *in vitro* evaluation using human cell lines. *J. Neuro-Oncol.*, **2008**, *86*, 165-72.
- [59] Liu, S.-Y.; Liang, Z.-S.; Gao, F.; Luo, S.-F.; Lu, G.-Q. *In vitro* photothermal study of gold nanoshells functionalized with small targeting peptides to liver cancer cells. *J. Mater. Sci.-Mater. Med.*, **2010**, *21*, 665-74.
- [60] O'Neal, D.P.; Hirsch, L.R.; Halas, N.J.; Payne, J.D.; West, J.L. Photo-thermal tumor ablation in mice using near infrared-absorbing nanoparticles. *Cancer Letters*, **2004**, *209*, 171-76.
- [61] Gobin, A.M.; Lee, M.H.; Halas, N.J.; James, W.D.; Drezek, R.A.; West, J.L. Near-Infrared Resonant Nanoshells for Combined Optical Imaging and Photothermal Cancer Therapy. *Nano. Letters.*, **2007**, *7*, 1929-34.
- [62] Huang, X.; El-Sayed, I.H.; Qian, W.; El-Sayed, M.A. Cancer Cell Imaging and Photothermal Therapy in the Near-Infrared Region by Using Gold Nanorods. *J. Am. Chem. Soc.*, **2006**, *128*, 2115-20.
- [63] Sau, T.K.; Murphy, C.J. Seeded High Yield Synthesis of Short Au Nanorods in Aqueous Solution. *Langmuir*, **2004**, *20*, 6414-20.
- [64] Gou, L.; Murphy, C.J. Fine-Tuning the Shape of Gold Nanorods. *Chem. Mat.*, **2005**, *17*, 3668-72.
- [65] Kooij, S.; Poelsema, E.; Bene. Shape and size effects in the optical properties of metallic nanorods. *Phys. Chem. Chem. Phys.*, **2006**, *8*, 3349-57.
- [66] Murphy, C.J.; Sau, T.K.; Gole, A.M.; Orendorff, C.J.; Gao, J.; Gou, L.; Hunyadi, S.E.; Li, T. Anisotropic Metal Nanoparticles: Synthesis, Assembly, and Optical Applications. *J. Phys. Chem. B*, **2005**, *109*, 13857-70.
- [67] SK, K.; S, C.; CY, Y.; J, Y. Aspect Ratio Controlled Synthesis of Gold Nanorods. *Korean Journal of Chemical Engineering*, **2003**, *20*, 1145-48.
- [68] Dickerson, E.B.; Dreaden, E.C.; Huang, X.; El-Sayed, I.H.; Chu, H.; Pushpanketh, S.; McDonald, J.F.; El-Sayed, M.A. Gold nanorod assisted near-infrared plasmonic photothermal therapy (PPTT) of squamous cell carcinoma in mice. *Cancer. Letters.*, **2008**, *269*, 57-66.
- [69] Chou, C.-H.; Chen, C.-D.; Wang, C.R.C. Highly Efficient, Wavelength-Tunable, Gold Nanoparticle Based Optothermal Nanoconvertors. *J. Phys. Chem. B*, **2005**, *109*, 11135-38.
- [70] Jang, B.; Kim, Y.S.; Choi, Y. Effects of Gold Nanorod Concentration on the Depth-Related Temperature Increase During Hyperthermic Ablation. *Small*, **2011**, *7*, 265-70.
- [71] Chen, J.; Glaus, C.; Laforest, R.; Zhang, Q.; Yang, M.; Gidding, M.; Welch, M.J.; Xia, Y. Understanding the Photothermal Conversion Efficiency of Gold Nanocrystals. *Small*, **2010**, *6*, 2272-80.
- [72] Goodrich, G.P.; Bao, L.; Gill-Sharp, K.; Sang, K.L.; Wang, J.; Payne, J.D. Photothermal therapy in a murine colon cancer model

- using near-infrared absorbing gold nanorods. *Biomed. Opt.* **2010**, *15*, 018001.
- [73] Choi, J.; Yang, J.; Park, J.; Kim, E.; Suh, J.-S.; Huh, Y.-M.; Haam, S. Specific Near-IR Absorption Imaging of Glioblastomas Using Integrin-Targeting Gold Nanorods. *Adv. Funct. Mater.*, **2011**, *21*, 1082-88.
- [74] Schwartzberg, A.M.; Olson, T.Y.; Talley, C.E.; Zhang, J.Z. Synthesis, Characterization, and Tunable Optical Properties of Hollow Gold Nanospheres†. *J. Phys. Chem. B*, **2006**, *110*, 19935-44.
- [75] Sun, Y.; Mayers, B.; Xia, Y. Metal Nanostructures with Hollow Interiors. *Adv. Mater.*, **2003**, *15*, 641-46.
- [76] Skrabalak, S.E.; Chen, J.; Sun, Y.; Lu, X.; Au, L.; Cobley, C.M.; Xia, Y. Gold Nanocages: Synthesis, Properties, and Applications. *Accounts Chem. Res.*, **2008**, *41*, 1587-95.
- [77] Lu, W.; Xiong, C.; Zhang, G.; Huang, Q.; Zhang, R.; Zhang, J.Z.; Li, C. Targeted Photothermal Ablation of Murine Melanomas with Melanocyte-Stimulating Hormone Analog-Conjugated Hollow Gold Nanospheres. *Clin. Cancer Res.*, **2009**, *15*, 876-86.
- [78] Lu, X.; Chen, J.; Skrabalak, S.E.; Xia, Y. Galvanic replacement reaction: a simple and powerful route to hollow and porous metal nanostructures. *Proceedings of the Institution of Mechanical Engineers, Part N: Journal of Nanoengineering and Nanosystems*, **2007**, *221*, 1-16.
- [79] Au, L.; Zheng, D.; Zhou, F.; Li, Z.-Y.; Li, X.; Xia, Y. A Quantitative Study on the Photothermal Effect of Immuno Gold Nanocages Targeted to Breast Cancer Cells. *ACS Nano*, **2008**, *2*, 1645-52.
- [80] Chen, J.; Wang, D.; Xi, J.; Au, L.; Siekkinen, A.; Warsen, A.; Li, Z.-Y.; Zhang, H.; Xia, Y.; Li, X. Immuno Gold Nanocages with Tailored Optical Properties for Targeted Photothermal Destruction of Cancer Cells. *Nano. Letters*, **2007**, *7*, 1318-22.
- [81] Skrabalak, S.E.; Chen, J.; Au, L.; Lu, X.; Li, X.; Xia, Y. Gold Nanocages for Biomedical Applications. *Adv. Mater.*, **2007**, *19*, 3177-84.
- [82] Chen, J.; Glaus, C.; Laforest, R.; Zhang, Q.; Yang, M.; Gidding, M.; Welch, M.J.; Xia, Y. Gold Nanocages as Photothermal Transducers for Cancer Treatment. *Small*, **2010**, *6*, 811-17.
- [83] El-Sayed, I.H.; Huang, X.; El-Sayed, M.A. Selective laser photothermal therapy of epithelial carcinoma using anti-EGFR antibody conjugated gold nanoparticles. *Cancer Lett.*, **2006**, *239*, 129-35.
- [84] Li, J.-L.; Wang, L.; Liu, X.-Y.; Zhang, Z.-P.; Guo, H.-C.; Liu, W.-M.; Tang, S.-H. *In vitro* cancer cell imaging and therapy using transferrin-conjugated gold nanoparticles. *Cancer Lett.*, **2009**, *274*, 319-26.
- [85] Norman, T.J.; Grant, C.D.; Magana, D.; Zhang, J.Z.; Liu, J.; Cao, D.; Bridges, F.; Van Buuren, A. Near Infrared Optical Absorption of Gold Nanoparticle Aggregates. *J. Phys. Chem. B*, **2002**, *106*, 7005-12.
- [86] Zhang, G.; Yang, Z.; Lu, W.; Zhang, R.; Huang, Q.; Tian, M.; Li, L.; Liang, D.; Li, C. Influence of anchoring ligands and particle size on the colloidal stability and *in vivo* biodistribution of polyethylene glycol-coated gold nanoparticles in tumor-xenografted mice. *Biomaterials*, **2009**, *30*, 1928-36.
- [87] Oli, M. Aptamer conjugated gold nanorods for targeted nanothermal radiation of Glioblastoma cancer cells (A novel selective targeted approach to cancer treatment). *Young Scientists Journal*, **2010**, *3*, 18-25.
- [88] De Jong, W.H.; Hagens, W.I.; Krystek, P.; Burger, M.C.; Sips, A.J.A.M.; Geertsma, R.E. Particle size-dependent organ distribution of gold nanoparticles after intravenous administration. *Biomaterials*, **2008**, *29*, 1912-19.
- [89] erentyuk, G.S.; Maslyakova, G.N.; Suleymanova, L.V.; Khlebtsov, B.N.; Kogan, B.Y.; Akchurin, G.G.; Shantrocha, A.V.; Maksimova, I.L.; Khlebtsov, N.G.; Tuchin, V.V. Tuchin. Circulation and distribution of gold nanoparticles and induced alterations of tissue morphology at intravenous particle delivery. *J. Biophotonics*, **2009**, *2*, 292-302.
- [90] Shiotani, A.; Akiyama, Y.; Kawano, T.; Niidome, Y.; Mori, T.; Katayama, Y.; Niidome, T. Active Accumulation of Gold Nanorods in Tumor in Response to Near-Infrared Laser Irradiation. *Bioconjugate Chem.*, **2010**, *21*, 2049-54.
- [91] Kim, E.; Yang, J.; Choi, J.; Suh, J.-S.; Huh, Y.-M.; Haam, S. Synthesis of gold nanorod-embedded polymeric nanoparticles by a nanoprecipitation method for use as photothermal agents. *Nanotechnology*, **2009**, *20*, 365602.
- [92] Alcantar, N.A.; Aydil, E.S.; Israelachvili, J.N. Polyethylene glycol-coated biocompatible surfaces. *J. Biomed. Mater. Res. Part A*, **2000**, *51*, 343-51.
- [93] Perrault, S.D.; Walkey, C.; Jennings, T.; Fischer, H.C.; Chan, W.C.W. Mediating Tumor Targeting Efficiency of Nanoparticles Through Design. *Nano Letters*, **2009**, *9*, 1909-15.
- [94] Jiang, W.; KimBetty, Y.S.; Rutka, J.T.; ChanWarren, C.W. ChanWarren. Nanoparticle-mediated cellular response is size-dependent. *Nat. Nano.*, **2008**, *3*, 145-50.
- [95] Jain, R.K. Transport of Molecules, Particles, and Cells in Solid Tumors. *Annu. Rev. Biomed. Eng.*, **1999**, *1*, 241-63.
- [96] Pluen, A.; Netti, P.A.; Jain, R.K.; Berk, D.A. Diffusion of Macromolecules in Agarose Gels: Comparison of Linear and Globular Configurations. *Biophys. J.*, **1999**, *77*, 542-52.
- [97] Weissleder, R.; Ntziachristos, V. Shedding light onto live molecular targets. *Nat. Med.*, **2003**, *9*, 123-28.
- [98] Schwartz, J.A.; Shetty, A.M.; Price, R.E.; Stafford, R.J.; Wang, J.C.; Uthamanthil, R.K.; Pham, K.; McNichols, R.J.; Coleman, C.L.; Payne, J.D. Feasibility Study of Particle-Assisted Laser Ablation of Brain Tumors in Orthotopic Canine Model. *Cancer Res.*, **2009**, *69*, 1659-67.
- [99] von Maltzahn, G.; Park, J.-H.; Agrawal, A.; Bandaru, N.K.; Das, S.K.; Sailor, M.J.; Bhatia, S.N. Computationally Guided Photothermal Tumor Therapy Using Long-Circulating Gold Nanorod Antennas. *Cancer Research*, **2009**, *69*, 3892-900.
- [100] Vera, J.; Bayazitoglu, Y. Gold nanoshell density variation with laser power for induced hyperthermia. *Int. J. Heat Mass Transf.*, **2009**, *52*, 564-73.
- [101] Li, J.L.; Day, D.; Gu, M. Ultra-Low Energy Threshold for Cancer Photothermal Therapy Using Transferrin-Conjugated Gold Nanorods. *Adv. Mater.*, **2008**, *20*, 3866-71.
- [102] Huang, X.; Qian, W.; El-Sayed, I.H.; El-Sayed, M.A. The potential use of the enhanced nonlinear properties of gold nanospheres in photothermal cancer therapy. *Lasers Surg. Med.*, **2007**, *39*, 747-53.